0273-2289/01/94/0179/$14.50

Application of Near-Infrared Spectra on Temperature-Controlled Protein Crystallization

A Simulation Study

Shih-Yao B. Hu,*[,1] John M. Wiencek,[1] and Mark A. Arnold[2]

[1]Department of Chemical and Biochemical Engineering and Center of Optical Science and Technology and [2]Department of Chemistry and Center of Optical Science and Technology, University of Iowa, 280 IATL, Iowa City, IA 52242
E-mail: barry-hu@uiowa.edu

Received August 1, 2000; Accepted February 1, 2001

Abstract

Large, high-quality protein crystals are required for the structural determination of proteins via X-ray diffraction. In this article, we propose a technique to facilitate the production of such crystals and validate its feasibility through simulations. An analytical method for protein aqueous solution based on a Fourier transform infrared (FTIR) spectroscopy is combined with a temperature control strategy to manipulate the extent of supersaturation during crystal growth, thus impacting crystal quality. The technique requires minimal knowledge about the growth kinetics *a priori*. The simulations show that, under ideal conditions, the design can be as effective as predesigned temperature programs for crystallization based on known growth kinetics. Two kinds of errors might be encountered with this design. Error in the estimated number of seed crystals can result in a growth rate deviating from the desired one. Nevertheless, the deviation is usually tolerable and system instability is unlikely to occur. Based on the standard error of our FTIR method, errors in concentration measurement are simulated. Measurement error can result in system instability and impair the control algorithm. Such errors may be compensated by limiting the temperature change taken by the control action, or by improving the measurement precision through the use of regressed concentrations. Through simulations, it is shown that the proposed design is practical and represents a significant improvement over the commonly used isothermal crystallization technique.

*Author to whom all correspondence and reprint requests should be addressed.

Index Entries: Protein crystallization; simulation; Fourier transform infrared, lysozyme.

Introduction

Large, well-formed crystals are essential for successful X-ray crystallographic structure determinations. Crystal of such quality can be obtained by controlling the level of supersaturation during the crystallization process *(1)*. In protein crystallization, supersaturation is normally controlled through the use of precipitants or pH. Typically, protein in a hanging drop is equilibrated against a reservoir of precipitant solution of higher concentration to produce protein crystals. Such a design provides no control over the level of supersaturation beyond setting the initial conditions. As a result, growing high-quality crystals has largely been a trial-and-error process. Efforts have been made to control supersaturation during the growth of protein crystal. For example, Gernert et al. *(1)* devised a hanging-drop apparatus in which the reservoir concentration could be changed over time and found that maintaining a lower level of supersaturation led to fewer protein crystals of larger size than crystals grown under highly supersaturated conditions.

An alternative approach to regulate supersaturation is through temperature control. Such a method has been practiced on inorganic crystallization for years *(2)*, but only recently have studies utilized this strategy to control nucleation and growth of protein crystals *(3–8)*. Conceptually, as protein in the liquid phase is consumed during crystallization, the corresponding change in supersaturation is compensated by a change in temperature since solubility is temperature dependent. Although shown effective, this method has been underutilized because it requires knowledge of the solubility as a function of temperature along with nucleation and growth kinetics.

A new approach combining temperature control and on-line concentration monitoring is proposed here. By measuring changes in soluble protein concentration, one can calculate the crystal growth rate through a simple mass balance. This growth rate can then be utilized within a control algorithm that will adjust the system temperature according to the difference between the detected growth rate and the targeted growth rate. Only minimal knowledge is required about the protein. Such a technique requires a sensitive, temperature-independent analytical method for protein solutions; a robust control algorithm; and an efficient temperature control mechanism.

We have established the feasibility of such an approach by developing an analytical method for protein aqueous solution with Fourier transform infrared (FTIR) spectroscopy *(9)*. The most common method for measuring protein concentrations is to use light absorbance at 280 nm on ultraviolet spectrometers. However, the high energy of such light sources can damage the peptide bonds of protein molecules and is therefore not suitable for long-term, continuous measurements *(10)*. By utilizing digital Fourier fil-

tering, our FTIR method is temperature independent, unlike typical FTIR methods; calibration generated at a single temperature can be used to calculate sample concentrations over a wide range of temperature with a root mean square error of calibration of 0.195 mg/mL for lysozyme. A detection limit of 0.68 mg/mL is achieved and a linear response is obtained up to 51 mg/mL.

In the present study, we implement a temperature control algorithm for protein crystallization based on this FTIR method. The algorithm is tested on lysozyme, a well-characterized protein, through simulations. The effectiveness of the design is examined under various conditions.

Theory

The growth rate, G (μm/h), of a protein crystal is defined as the change in length, ΔL (μm), in one arbitrary dimension of the crystal over a period of time Δt (h):

$$G = \Delta L / \Delta t \tag{1}$$

The overall mass, m (mg), of crystals in a system is calculated by

$$m = N \cdot \rho_{eff} \cdot k_v \cdot (L/1000)^3 \tag{2}$$

in which N is the number of crystals in the system, ρ_{eff} (mg of protein/mL of crystal volume) is the density of the crystal, and k_v is the shape factor of the crystal. The shape of lysozyme crystal is approximated by a cube, and k_v has a value of 8 provided L is defined as the center-to-edge distance.

The relationship between solubility and temperature can be characterized by the van't Hoff equation (8):

$$\ln C^* = \frac{\Delta H_{cryst}}{R}\left(\frac{1}{T} - b\right) \tag{3}$$

in which C^* (mg/mL) is the protein solubility, ΔH_{cryst} (kcal/mol) is the enthalpy of formation of crystals, R (0.001986 kcal/[mol·K]) is the ideal gas constant, T(K) is the system temperature, and b(1/K) is an empirical constant. Equation 3 shows that the solubility decreases as temperature decreases if the crystallization is an exothermal process ($\Delta H_{cryst} < 0$), which is the case for lysozyme. A power law growth model is often adequate for quantifying the growth kinetics:

$$G = 60 \cdot k \cdot (C - C^*)^n \tag{4}$$

in which k ([μm/min]/[mg/mL]^n) and n are empirical constants. Values of k and n for both the [110] and [101] faces have been determined experimentally for a variety of tetragonal lysozyme crystallization conditions *(11)*.

In addition to the definition Eq. 1 , geometry Eq. 2, thermodynamics Eq. 3, and kinetics Eq. 4, a mass balance equation can be written for the system:

$$m = m_{ini} + (C_{ini} - C) \cdot V \tag{5}$$

in which m_{ini} (mg) is the mass of seed crystals, C_{ini} (mg/mL) is the initial soluble protein concentration, and V (mL) is the volume of the liquid phase. Equations 1–5 construct our model for protein crystal growth.

Simulations and Discussions

All the simulations conducted are based on a 12 mg/mL lysozyme solution in 0.1 *M* acetate buffer at pH 4.6 with 5 w/v% sodium chloride. Such solution conditions are commonly utilized to grow lysozyme crystals *(11)*. The values of ΔH_{cryst}, b, k, and n for this system are –14.6 kcal/mol, 0.003664 K^{-1}, 0.004 (μm/min)/(mg/mL)^n, and 1.4, respectively, and a density ρ_{eff} of 720 mg/mL and a shape factor k_v of 8 are used *(12)*. Unless otherwise specified, the number of crystals, N, is assumed to be 20, and the volume of the liquid phase, V, is assumed to be 0.6636 mL. Seed crystal mass, m_{ini}, is assumed to be 0, which corresponds to an infinitely small nucleus. The targeted growth rate, G_{set}, is set to 1 μm/h and the initial temperature is set to 25°C. The simulations were carried out on Microsoft Excel spreadsheets. In all the figures except Fig. 8, growth rate is represented by a solid line, temperature is represented by a dashed line, and concentration is represented by a dotted line.

Isothermal Growth

Typically, protein crystals are grown under isothermal conditions. As mentioned earlier, such a design provides no control over the level of supersaturation beyond setting the initial conditions. This isothermal experiment is simulated with known crystallization kinetics and thermodynamics. Two such examples are shown in Fig. 1. Figure 1A shows the isothermal growth at 4°C. As expected, the initial growth rate is high because of the high extent of supersaturation. Such a fast-growing condition usually results in crystals of poor quality, as shown in the inset *(8)*. In addition, both nucleation and growth occur under such conditions. The many nuclei consume the mass of protein and lead to many small crystals. Such small, defective crystals are undesirable for X-ray diffraction studies. Figure 1B shows the isothermal growth at 25°C. Under this condition, the growth rate is maintained under 0.75 μm/h. Although this is favorable for producing high-quality crystals, the overall reduction in the soluble protein concentration is small (from 12 to about 10 mg/mL). This means that most of the protein molecules are still in the liquid phase. The resultant crystal will be small, which also is not desirable for X-ray diffraction study.

Predicted Optimal Temperature Profile

When the values of ΔH_{cryst}, b, k, and n are known for a system, one can calculate a temperature, T_{set} (K), required to achieve a targeted growth rate, G_{set} (μm/h), by combining Eqs. 3 and 4:

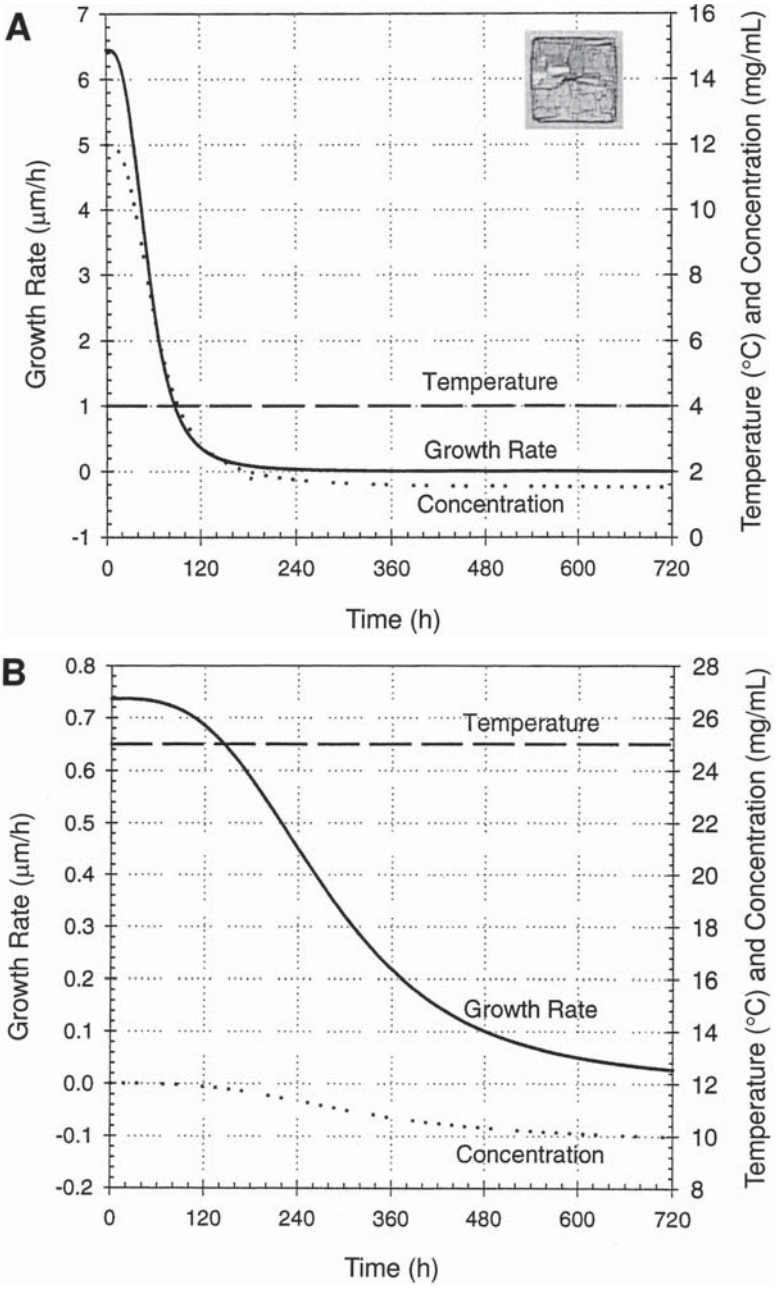

Fig. 1. Isothermal crystallization of lysozyme at **(A)** 4°C and **(B)** 25°C. Fast growth rate at 4°C results in defective crystals, as shown in the inset. Small conversion at 25°C results in small crystals. Neither is ideal for X-ray crystallography *(8)*.

$$T_{set} = \frac{\Delta H_{cryst}}{R} \left\{ \frac{1}{\ln [C - (G_{set}/60 \cdot k)^{1/n}] + b} \right\} \quad (6)$$

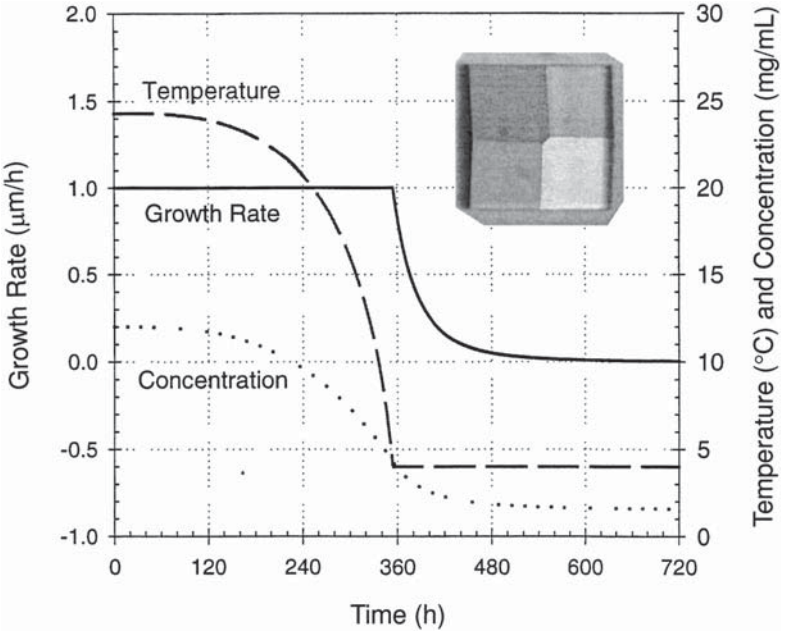

Fig. 2. Lysozyme crystallization based on a predesigned temperature profile. A slow growth rate is maintained throughout the process. The resultant crystals are larger and macroscopically defect free, as shown in the inset *(8)*.

An optimal temperature profile for crystallization can be derived from the following algorithm:

1. Start with initial concentration, C_{ini}, and desired growth rate, G_{set}, and calculate the optimal temperature T_{set}, with Eq. 6.
2. Calculate the size of the crystals after a period Δt with Eq. 1, then the overall mass of crystals, m, with Eq. 2.
3. Calculate the new concentration, C, with Eq. 5.
4. Repeat steps 1–3 until the desirable time has been reached.

Two points need to be addressed about this algorithm. First, the method is explicit mathematically; it calculates the new conditions based solely on the previous conditions. The concentration is assumed to remain constant throughout the period Δt. An implicit method may be established by incorporating the new concentration in a log-mean form and solved through iterations. However, since the concentration changes in such a system are usually very slow, the error introduced by using explicit formula is negligible. Second, some physical limits need to be imposed on the algorithm. For example, a temperature too low may freeze the aqueous solution; a high temperature can accelerate the denaturation of the protein molecules. The temperature is limited between 4 and 30°C in all the simulations.

Figure 2 shows a designed temperature profile based on known kinetics and thermodynamics of crystallization. The growth rate is perfectly

controlled at the set point of 1 µm/h until the lower temperature limited was reached at about 360 h. The concentration and temperature change slowly initially and then drop quickly after 240 h, because the growth rate is defined on a linear scale whereas the increase in crystal size is three dimensional; as the surface area of crystals increases with crystal growth, more molecules need to crystallize to maintain a constant linear growth rate. When the temperature hits the minimum limit, the growth rate can no longer be controlled and the process simply relaxes at 4°C. An inflection point in the concentration curve occurs at this sample time. The size of the resultant crystals after 720 h is calculated to be 392 µm (assuming 20 crystals are formed). A sample lysozyme crystal grown under controlled temperature profile is shown in the inset of Fig. 2 *(8)*.

Growth Rate Control with On-Line Concentration Measurements

When the kinetics and thermodynamics of crystal growth are not known for a system, it is still possible to achieve a desired growth rate through on-line concentration monitoring and feedback control. The concept is simple: by measuring concentration, C, one can calculate the overall crystal mass, *m*, with Eq. 5 and the crystal size with Eq. 2. The growth rate is calculated with Eq. 1 and then normalized through the following equation:

$$\Gamma = [(G - G_{set})/G_{set}] \tag{7}$$

Γ, the normalized growth rate, gives a better indication of how far the current condition is from the set point than the growth rate, *G*, does; a Γ of 0 represents perfect control while the sign and value of Γ tells us whether we have a positive or negative deviation. Γ is fed to a PID control (proportional plus reset plus rate control *[13]*) algorithm to adjust system temperature, *T*, to $T + \Delta T$:

$$\Delta T = -\text{sign}(\Delta H_{cryst}) \cdot \left(K_p \cdot \Gamma + K_i \cdot \sum \Gamma \cdot \Delta t + K_d \frac{\Delta \Gamma}{\Delta t} \right) \tag{8}$$

in which $-\text{sign}(\Delta H_{cryst})$ gives the direction of adjustment. For example, when $\Delta H_{cryst} < 0$ (solubility increases with temperature), $-\text{sign}(\Delta H_{cryst})$ equals +1; if a positive deviation is observed (growth rate higher than the set point), temperature should be increased ($\Delta T > 0$) to increase the solubility and decrease the driving force ($C - C^*$). K_p, K_i, and K_d are the proportional, integral, and derivative control constants, respectively. The three terms compensate the current deviation, accumulated deviation, and change in deviation, respectively. With this design, the only information required to control the crystal growth rate during a crystallization process would be the sign of ΔH_{cryst} and estimates of density, ρ_{eff}, and shape factor, k_v.

Figure 3 shows the result from the simulation using on-line concentration measurement and PID feedback control. The system response is almost

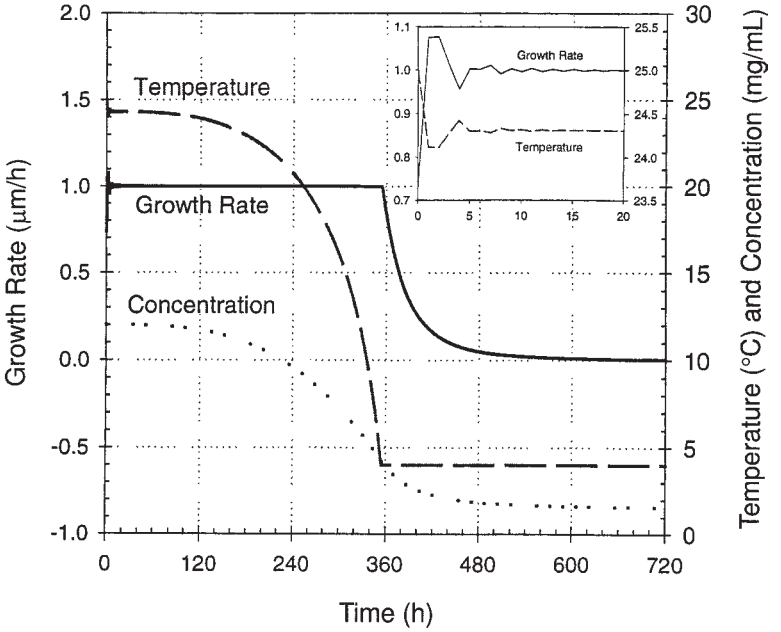

Fig. 3. Temperature-controlled lysozyme crystallization based on input from on-line concentration measurements. The profile is nearly identical to a predesigned one (Fig. 2). The fluctuation at the beginning, enlarged in the inset, is small and will not impact the quality of the crystal.

identical to the one based on the predicted optimal temperature profile. The deviation in the growth rate is perceptible only at the initiation of the experiment, because the initial temperature (25°C) is relatively far away from the optimal temperature (24.31°C) and the control algorithm requires several steps to adjust the temperature to optimal. The control parameters K_p, K_i, and K_d have been optimized to be 3.36, 5.42, and 0.74, respectively, using the Solver functionality of Excel to minimize the objective function:

$$\sum \Gamma^2 \Big| T > T_{min} \tag{9}$$

That is, the sum of the square of the normalized growth rate, Γ, for each step as long as the temperature has not reached the minimum. As defined in Eq. 7, a "perfect" control should maintain a Γ of 0. Thus, the sum of square of Γ should be as small as possible. These parameters can be optimized only if the kinetic and thermodynamic parameters of crystallization are known. Although this optimization operation cannot be applied to a less-characterized system, the feasibility of our approach is clearly demonstrated.

Error in Estimating Number of Seed Crystals

Two possible errors may be encountered with our control strategy: error in estimating the number of seed crystals and error in measuring the

protein concentrations. Crystals must grow from nuclei. In practice, these nuclei may be generated separately and then transferred, or "seeded," to the crystallization system. In this case, the number of seed crystals can be quantified correctly. Alternatively, one can lower the system temperature such that the system enters the labile zone and nucleation occurs. The exact number of seed crystals formed by this means is usually difficult to determine. This error obviously can impact the effectiveness of the control strategy. Another source of error is from the concentration measurements, which are discussed in more detail in later sections. To incorporate these errors, the algorithm for simulation is modified as follows:

1. Start with initial concentration, C_{ini}, and temperature, T_{ini}, and calculate the concentration after Δt using Eqs. 3, 4, 1, then 2.
2. Add measurement error to the calculated concentration through a random number generator based on a student's t distribution. The new concentration is represented by C'.
3. Calculate overall crystal mass m' with Eq. 5 and then use in Eq. 2 to calculate crystal size L'. An inaccurate number of crystals N', is incorporated in this step. Then calculate the inaccurate, normalized growth rate, Γ', using Eqs. 1 and 7.
4. Assume no knowledge about the system and adjust the temperature according to Eq. 8.
5. Simulate the outcome of the adjustment made in step 3 after Δt with Eqs. 1–4.
6. Repeat steps 2–5.

Two examples shown in Fig. 4 demonstrate what could happen when the number of seed crystals is overestimated and underestimated. The control parameters were reoptimized. When the number of seed crystals is overestimated by a factor of 2, the controlled growth rate is higher than the targeted growth rate by about 26%. Underestimating the number of seed crystals by three-fourths results in a growth rate about 37% lower than the set point. In either case, the control remains effective and no instability is observed. Even with these possible deviations, the growth rate control is far better than the typically used isothermal conditions, as shown in Fig. 1. The same result may be derived mathematically based on the predicted optimal temperature profile:

$$G' = G_{set}\left(\frac{N'}{N}\right)^{1/3} \tag{10}$$

Overestimating N by an order of magnitude will result in a growth rate increases of about twofold. Although such an increase might not significantly deteriorate crystal quality, it is obvious that a conservative estimate ($N' < N$) is desirable. A wrong N' does not significantly effect the system's control stability.

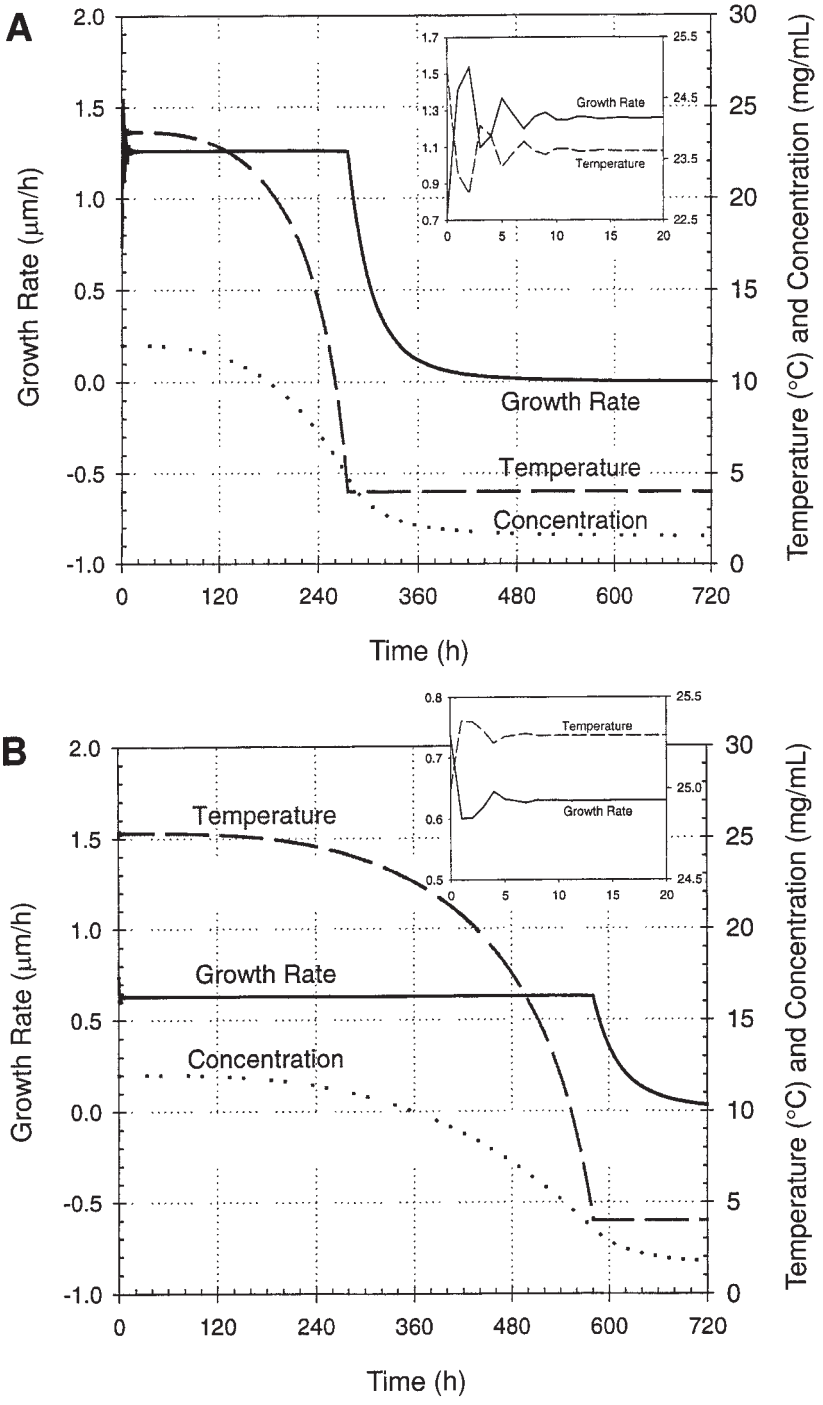

Fig. 4. Effect of error in estimating number of seed crystals: **(A)** overestimating number of seed crystals; $N = 20$, $N' = 40$; **(B)** underestimating number of seed crystals; $N = 20$, $N' = 5$. The insets show a detailed view of the initial fluctuation. In both cases, the control is still effective, and the growth rates are maintained reasonably well.

Measurement Errors

Measurement error is inevitable in any analytical method and must be considered if the control strategy is highly sensitive to the concentration. To incorporate measurement errors into the simulations, we started with the linear calibration model used in our FTIR method:

$$A = b_0 + b_1 \cdot C \tag{11}$$

in which A is the integrated peak area of FTIR spectra and b_0 and b_1 are the intercept and slope of the regression line, respectively. A $100(1 - \alpha)\%$ confidence interval for a single measurement may be characterized by *(14)*

$$C' = C \pm t_{\alpha/2} \cdot \sigma \cdot \sqrt{1 + \frac{1}{M} + \frac{(b_0 + b_1 \cdot C - \overline{A})^2}{S_{AA}}} \tag{12}$$

in which C' is the concentration from FTIR analysis (in contrast to the real concentration C), $t_{\alpha/2}$ is the student's t statistic, σ is the standard error of calibration (SEC), M is the calibration sample number, $\overline{A}$ is the average peak area of all calibration sample spectra, and

$$S_{AA} = \sum (b_0 + b_1 \cdot C - \overline{A})^2 \tag{13}$$

is the sum of square of peak area from the calibration sample spectra. A random number generator based on the probability distribution of $t_{\alpha/2}$ is used to simulate the measurement errors. An α of 0.05 (a 95% confidence interval) was used in all the simulations. The calibration model used is based on previous work by us, in which an SEC of 0.195 mg/mL was obtained *(9)*.

Figure 5 shows the effect of measurement error on the temperature control. The proportional control constant K_p is reduced to 0.1 because the system is highly unstable at a higher K_p. Both proportional and derivative constants (K_i and K_d) have been set to zero. Parameter optimization at this level of measurement error is ineffective. Basically, the temperature fluctuates between the limits, 4 and 30°C, initially. Had these limits not been imposed, the system would act even more erratic. These two temperatures translate into growth rates of about –1 and 6.5 µm/h, respectively. It is possible to reduce K_p further to reduce the temperature fluctuation, but the control would not be robust. A closer inspection on the spreadsheet reveals that a perfect temperature control (Fig. 3) requires the detection of a concentration change of 6.93784E-08 mg/mL in a 12 mg/mL solution after the first hour of the experiment; a temperature adjustment of –0.039511452°C is made accordingly. A spectroscopic method that can achieve such a high precision is unlikely to exist. Temperature control at such a small magnitude is also difficult. Obviously, some adjustments need to be made for the control strategy to be effective.

A possible alternative is to adjust the temperature passively. That is, the temperature will not be adjusted until a significant concentration change

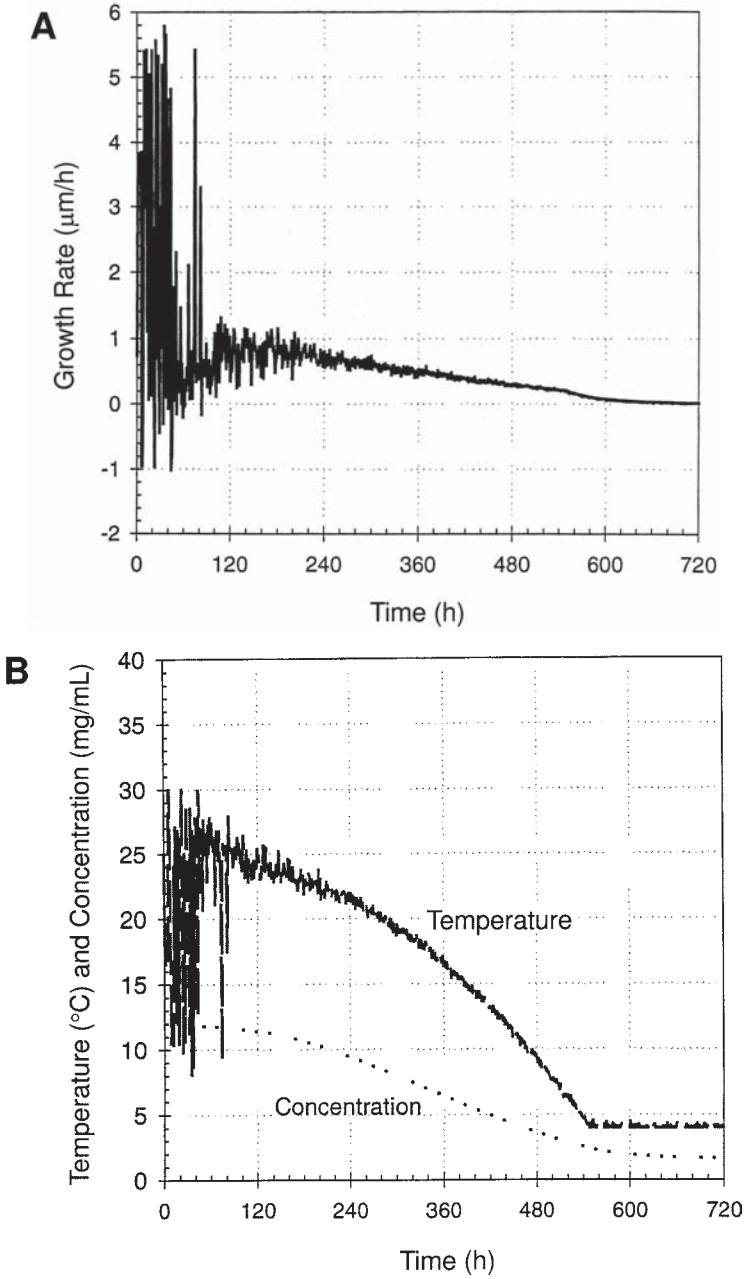

Fig. 5. Effect of error in measurements: **(A)** growth rate; **(B)** temperature and concentration. Measurement error impairs the control algorithm and results in system instability.

is detected. The result from simulation is shown in Fig. 6. The same random errors and the same control parameters as in Fig. 5 are used. It can be seen that the system is frequently stranded in near steady states in which the growth rate becomes so slow that the concentration does not change signifi-

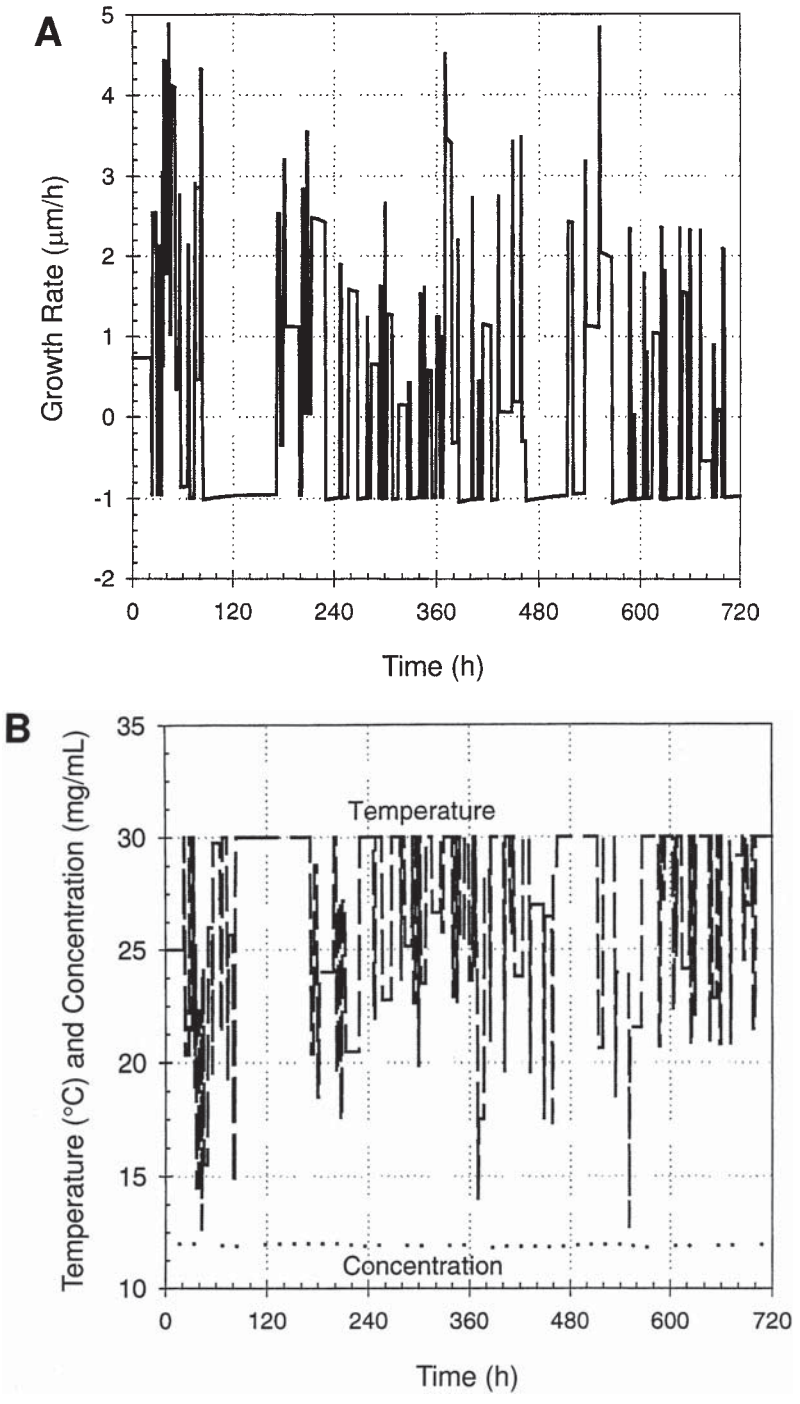

Fig. 6. Passive temperature control: **(A)** growth rate; **(B)** temperature and concentration. In passive temperature control, system temperature is not adjusted until a statistically significant change in concentration is detected. The system is trapped in a near steady state with almost no conversion. Measurement error is not compensated and system instability remains a problem.

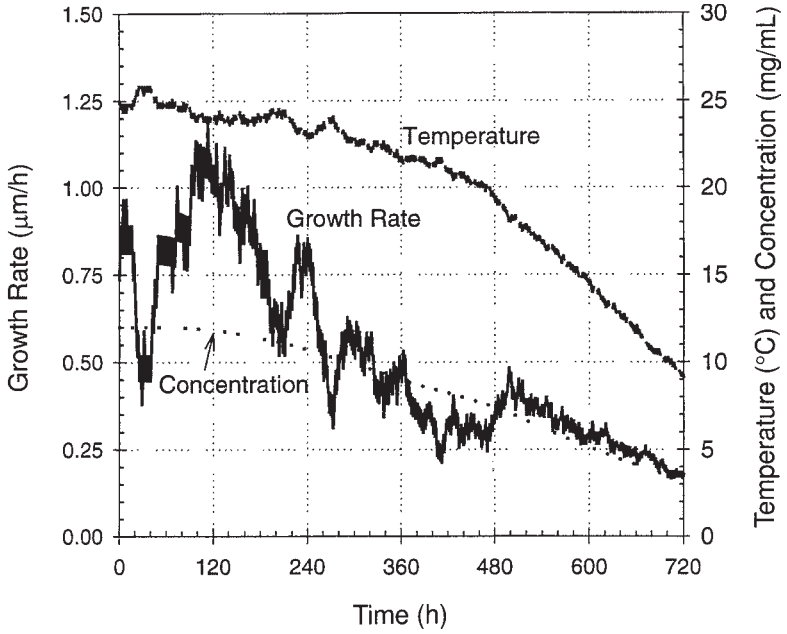

Fig. 7. Control with limited temperature adjustment. By limiting the scale of temperature adjustment, system instability is avoided and growth rate is controlled reasonably well. However, if the initial growth rate is far from the set point, the control cannot make robust adjustment to correct the growth condition.

cantly for a long period of time, and, therefore, no temperature adjustment is made. The fluctuation in temperature and growth rate is still notable and the net change in concentration is very small. Apparently, this scheme is inappropriate for our purpose as well.

Our third option is to limit the scale over which temperature can be adjusted in each step. With such a damping, instability should no longer be a problem. The random error in measurement can still cause temperature adjustment in the wrong direction in a single step. However, as long as the errors are random, the trend in concentration change should be revealed by the measurement over time, and the control will move in the correct direction. An example is shown in Fig. 7. Again the same errors and K_p as in Fig. 5 are used, and a limit of 0.2°C change in each step is imposed. Essentially, the temperature is adjusted 0.2°C every time so that the control parameters do not have any actual impact on the system. The growth rate is controlled below 1.20 μm/h. Although the growth rate control is satisfactory, the response is not as robust; at the end of 720 h, the temperature was reduced only to 9°C instead of the optimal value of 4°C. Such a behavior presents a potential problem: if the initial temperature produces a growth rate that is far from the target value, the control algorithm might not be able to adjust the temperature fast enough to obtain a reasonable growth rate. It is possible to compensate for this problem by increasing the limit of temperature adjustment, but the fluctuation in temperature and growth

rate would increase as well. Nevertheless, this is an algorithm worth considering.

Precision of analysis can be improved by taking the average of multiple measurements. Although this is possible for our application, a correct implementation would be hard to achieve. It takes about 1 min and 45 s to collect a spectrum on FTIR. This means that up to 34 spectra can be collected during a typical time interval of 1 h. The concentration is changing during the collection of these spectra. A simple average cannot reflect these changes, and it would be just as hard to determine when and how a moving average should be taken. A possible way to take advantage of increased precision with multiple replicates is to take a smooth curve fit over time to determine the concentration. Since the change is typically small over an hour, a simple linear curve fit should be able to reflect the concentration change. Figure 8 shows two examples of obtaining concentrations using linear regression. The concentration is continuously measured (open circles). At the end of an hour, a linear regression is carried out using all of the data collected in the past hour (solid line) and the concentration at the end of the hour is calculated. The time profile of real concentration (solid circles) is also shown. When the concentration change is very slow (Fig. 8A), such as in the early stage of a typical crystallization, curve-fitted concentration does not show a significant advantage over a simple average. However, when the concentration changes relatively fast (Fig. 8B), as in the later stage of crystallization, it is obvious that a curve-fitted concentration can reflect changes as well as improve measurement precision. If a 3- or 5-point moving average were used, error would not be significantly reduced; if a simple average were taken, the change would be smeared out and not accurately reflected in the results. Using this control technique, a temperature profile is shown in Fig. 9. Again the same K_p as in Fig. 5 is used and no limit in temperature adjustment is imposed. The growth rate is satisfactorily controlled between –1 and 3 μm/h compared to isothermal conditions (Fig. 1). It is more robust compared to the case of limited temperature adjustment (Fig. 7) and shows greater stability over a simple control (Fig. 5). No attempt was made to reoptimize K_p, K_i, and K_d because the precision, though vastly improved, is still far from ideal.

Conclusion

On-line FTIR analysis of protein solutions can be combined with a feedback, temperature control algorithm to control the growth rate of crystals during protein crystallization. The algorithm requires minimal knowledge about the protein being crystallized. Through simulations, it is shown that the algorithm can work as well as a predicted optimal temperature profile derived from known parameters of a well-characterized system such as lysozyme. Two possible errors are involved in this method: error in estimating the number of seed crystals and measurement error. Error in estimating the number of seed crystals can result in deviation of the con-

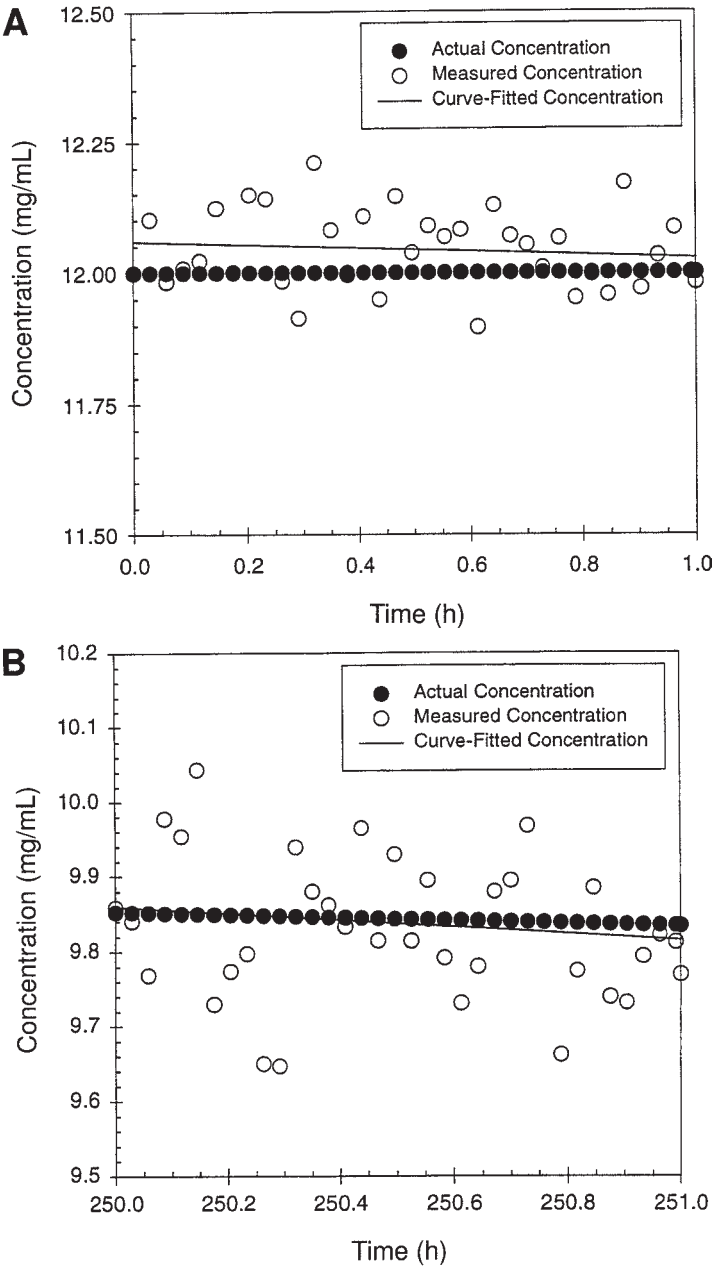

Fig. 8. Using curve-fitted concentration to improve measurement precision: **(A)** slow concentration change; **(B)** faster concentration change. The open circles are simulated measurements in which random errors based on the student's *t* distribution and standard error of calibration are incorporated. By using curve-fitted concentration, measurement precision is improved, and change in solute concentration is reflected.

trolled growth rate from the targeted growth rate. However, the deviation is usually tolerable and will not lead to instability of the system. Error in concentration measurements can lead to erratic temperature fluctuation

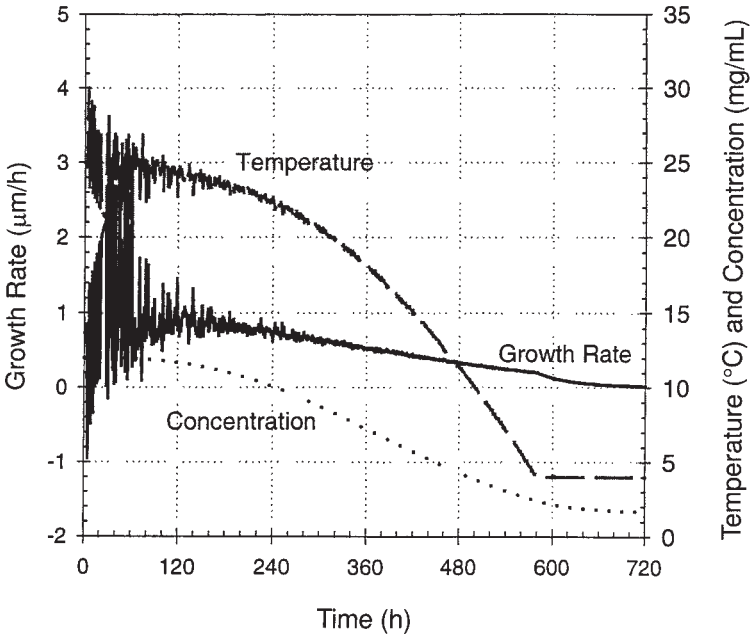

Fig. 9. Temperature control using curve-fitted concentration. With improved measurement precision, system instability is avoided. The growth rate is satisfactorily maintained near the set point.

and extreme growth rate and needs to be considered. A passive temperature-adjusting strategy that leaves the system unchanged until a significant concentration change is detected usually develops into near steady state and cannot effectively control the crystallization. Limiting the scale of temperature adjustment is a reasonable alternative, but the algorithm is less robust and is not likely to be effective when the initial temperature produces a growth rate far from the set point. The precision of measurement can be improved by collecting a series of concentration measurements and then calculating the concentration using a simple average or moving average. However, the change in concentration is not accurately reflected in such averaging techniques. Alternatively, linear regression can be used on the series of concentration measurements to reveal the concentration change while improving the precision. Our simulations show that the crystal growth rate can be controlled satisfactorily with this design. The system is stable and robust and it represents a great improvement over the commonly used isothermal methods.

Nomenclature

$\overline{A}$ = average peak area of all calibration sample spectra
A = integrated peak area of protein FTIR spectra
b = empirical constant in van't Hoff equation (1/K)
b_0, b_1 = coefficient of linear relation between A and C

C = soluble protein concentration (mg/mL)
C^* = solubility of protein (mg/mL)
G = growth rate of a crystal (μm/h)
k = proportional constant for crystal growth kinetics ([μm/min]/[mg/mL])^n
k_v = shape factor of crystals
L = length of a crystal (μm)
M = number of samples used in concentration calibration in FTIR method
m = overall mass of crystals (mg)
N = number of crystals
N' = estimation of number of crystals
n = power law constant for crystal growth kinetics
R = ideal gas constant (0.001986 kcal/[mol·K])
S_{AA} = sum of square of peak area from all calibration sample spectra
T = temperature (K)
t = time (h)
$t_{\alpha/2}$ = student's t distribution
V = liquid phase volume (mL)
ΔH_{cryst} = enthalpy of formation of crystals (kcal/mol)
ρ_{eff} = density of crystals (mg of protein/μm^3 of crystal volume)
σ = SEC in FTIR method

Subscript

$_{ini}$ = initial conditions

References

1. Gernert, K. M., Smith, R., and Carter, D. C. (1988), *Anal. Biochem.* **168,** 141–147.
2. Jones, A. G. and Mullin, J. W. (1974), *Chem. Eng. Sci.* **29,** 105–118.
3. DeMattei, R. C. and Feigelson, R. S. (1992), *J. Crystal Growth* **122,** 21–30.
4. Lorber, B. and Giegé, R. (1992), *J. Crystal Growth* **122,** 168–175.
5. Demattei, R. C. and Feigdelson, R. S. (1993), *J. Crystal Growth* **128,** 1225–1231.
6. Rosenberger, F., Howard, S. B., Sowers, J. W., and Nyce, T. A. (1993), *J. Crystal Growth* **90,** 1–12.
7. Bray, T. L., Kim, L. J., Askew, R. P., Harrington, M. D., Rosenblum, W. M., Wilson, W. W., and DeLucas, L. J. (1998), *J. Appl. Crystallogr.* **31,** 515–522.
8. Schall, C. A., Riley, J. S., Li, E., Arnold, E., and Wiencek, J. M. (1996), *J. Crystal Growth* **165,** 299–307.
9. Hu, S. B., Arnold, M. A., and Wiencek, J. M. (2000), *Anal. Chem.* **72,** 696–702.
10. Feher, G. and Kam, Z. (1985), *Methods Enzymol.* **114,** 77–112.
11. Durbin, S. D. and Feher, G. (1986), *J. Crystal Growth* **76,** 583–591.
12. Darcy, P. A. (1998), PhD thesis, University of Iowa, Iowa City, IA.
13. Wherry, T. C. and Miller, E. C. (1973), in *Chemical Engineer's Handbook*, 5th ed., Perry, R. H. and Chilton, C. H., eds., McGraw-Hill, New York, pp. 22-19–22-21.
14. Box, G. E. P., Hunter, W. G., and Hunter, J. S. (1978), in *Statistics for Experimenters*, John Wiley & Sons, New York, pp. 453–509.